Pharm Res (2012) 29:1392–1403
DOI 10.1007/s11095-012-0680-1

RESEARCH PAPER

Cellular Transfer of Magnetic Nanoparticles Via Cell Microvesicles: Impact on Cell Tracking by Magnetic Resonance Imaging

Amanda K. Andriola Silva • Claire Wilhelm • Jelena Kolosnjaj-Tabi • Nathalie Luciani • Florence Gazeau

Received: 25 August 2011 / Accepted: 6 January 2012 / Published online: 21 January 2012

ABSTRACT

Purpose Cell labeling with magnetic nanoparticles can be used to monitor the fate of transplanted cells *in vivo* by magnetic resonance imaging. However, nanoparticles initially internalized in administered cells might end up in other cells of the host organism. We investigated a mechanism of intercellular cross-transfer of magnetic nanoparticles to different types of recipient cells via cell microvesicles released under cellular stress.

Methods Three cell types (mesenchymal stem cells, endothelial cells and macrophages) were labeled with 8-nm iron oxide nanoparticles. Then cells underwent starvation stress, during which they produced microvesicles that were subsequently transferred to unlabeled recipient cells.

Results The analysis of the magnetophoretic mobility of donor cells indicated that magnetic load was partially lost under cell stress. Microvesicles shed by stressed cells participated in the release of magnetic label. Moreover, such microvesicles were uptaken by naïve cells, resulting in cellular redistribution of nanoparticles. Iron load of recipient cells allowed their detection by MRI.

Conclusions Cell microvesicles released under stress may be disseminated throughout the organism, where they can be uptaken by host cells. The transferred cargo may be sufficient to allow MRI detection of these secondarily labeled cells, leading to misinterpretations of the effectiveness of transplanted cells.

KEY WORDS cell microvesicles · cell tracking · magnetic nanoparticles · MRI

ABBREVIATIONS

BMSC	bone marrow stem cells
FBS	fetal bovine serum
FISP	fast steady state precession
FLASH	fast low-angle shot
HUVEC	human umbilical vascular endothelial cells
MSC	mesenchymal stem cells
PMA	phorbol 12-myristate 13-acetate
SWI	susceptibility weighted imaging

INTRODUCTION

Cell therapy has opened a wide field of resources for tissue regeneration and repair. However, in order to evaluate the therapeutic activity of cells, cell-tracking techniques are required to determine the fate of transplanted cells in both preclinical studies and clinical trials. In this concern, magnetic resonance imaging (MRI) offers the potential for non-invasive monitoring of transplanted cells (1).

A. K. A. Silva • C. Wilhelm • J. Kolosnjaj-Tabi • N. Luciani • F. Gazeau
Laboratoire Matière et Systèmes Complexes, UMR 7057
CNRS/Université Paris Diderot
Sorbonne Paris Cité
75205 Paris cedex 13, France

J. Kolosnjaj-Tabi
INSERM U970, Université Paris Descartes, Sorbonne Paris Cité
Paris Cardiovascular Research Center-PARCC/56 rue Leblanc
75737 Paris cedex 15, France

F. Gazeau (✉)
CNRS/Université Paris Diderot
Paris, France
e-mail: florence.gazeau@univ-paris-diderot.fr

MRI provides exhaustive three-dimensional (3D) functional and anatomic data, characterized by high soft-tissue contrast. The MRI technique does not require ionizing radiation, thereby it allows safe longitudinal follow-up for assessment of cell engraftment and migration. In order to visualize and distinguish implanted cells from resident tissues, cells have to be labeled with a contrast agent prior injection. Among the contrast agents, iron oxide-based nanoparticles have been proposed to label and track cells by MRI (2,3), especially because of their low toxicity, biodegradability and low impact on cell proliferation, differentiation and cell functionality (4).

In the follow-up of cellular therapy MRI should ideally combine high sensitivity, to detect a relatively small amount of cells, and high specificity, that is, any signal should be derived exclusively from viable, labeled cells (5). However, iron oxide nanoparticles may persist in the debris of labeled cells and may in turn produce a signal that can not be distinguished from the signal emitted by viable labeled cells, thus lead to overestimation of labeled cell engraftment (5).

In the past years, several research groups evidenced that different kinds of transplanted labeled stem cells may transfer their label to the macrophages of the host organism. As a result, hypointense signals in MRI analysis could represent a false positive for transplanted cells. Such persistence of MRI signal derived from ferumoxide-containing host cells suggests that MRI of magnetically labeled cells may not reliably report long-term follow-up of cell engraftment (5,6). To date, a number of studies pointed out the over interpretation of results from labeled transplanted cells, but enough attention was not drawn to the role of cell-released vesicles in the dissemination of the intracellular magnetic label content.

Cell microvesicles are released by most cell types during the processes of cell activation or during apoptosis. A number of studies demonstrated their implication in the transfer of biological information between cells at distance. Their involvement in physio-pathological processes, such as inflammation, pregnancy and blood coagulation, has been proven by several authors. Cell microvesicles can transport various molecules enclosed inside the vesicles or in their membrane, stemming from the parental cell that secretes them. Therefore "packages" of information can reach different cells, allowing distal cell communication (7–9).

In a recent study (10), we demonstrated that once internalized by mononuclear phagocyte cells, magnetic nanoparticles can also be released within microvesicles shed by activated or apoptotic cells. Membrane vesicles carry along magnetic nanoparticles to the extracellular space and are subsequently transferred to naïve macrophages after vesicle uptake. Intercellular transfer mediated by cell microvesicles results in the redistribution of the magnetic tag among macrophages.

Given this background, the driving hypothesis of this study was that vesicle-mediated transfer of intracellular magnetic nanoparticles to local cell hosts could account for the reported non-specific MRI signals while tracking magnetically labeled transplanted cells. This study therefore aimed to investigate the role of cell microvesicles in the transfer of magnetic nanoparticles *in vitro* under conditions of cellular stress induced by the serum-free cell culture medium. The transfer was studied among three different cell types: mesenchymal stem cells, endothelial cells and macrophages. At first we quantified the release of magnetic label from each type of cells. Subsequently we evaluated the redistribution of nanoparticle load between different cell types. Finally we wanted to ascertain that this intercellular transfer of nanoparticles is sufficient to enable detection of host cells by MRI.

MATERIALS AND METHODS

Cell Models

Human myelo-monocytic THP-1 cell line was cultured in suspension at a density of 0.2×10^6–1×10^6 cells/mL in RPMI 1640 medium containing 10% (v/v) fetal bovine serum, 2 mM L-glutamine and 100 U/mL penicillin-streptomycin, at 37°C in 5% CO_2. THP-1 monocytes (4×10^6 cells in 5 mL RPMI medium) were differentiated into macrophages by the treatment with phorbol ester (phorbol 12-myristate 13-acetate (PMA)) at a concentration of 50 ng/mL for 6 days.

Human umbilical vascular endothelial cells (HUVEC) line was cultured in EBM-2™ endothelial medium (Lonza) containing 2% fetal bovine serum (FBS) supplemented with EGM-2™ growth factor mixture (CC-4176, Lonza), according to the instructions of the supplier.

Mesenchymal stem cells (MSC) were cultured in MSCBM™ medium supplemented with MSCGM™ SingleQuot Kit (PT-4105, Lonza), also as specified by the supplier.

Cell Labeling with Magnetic Nanoparticles

Magnetic labeling was performed with 8-nm maghemite citrate-coated nanoparticles diluted to 10 mM iron concentration in serum-free RPMI medium supplemented with 5 mM sodium citrate (4). THP-1 macrophages, HUVEC and MSC underwent a 30-min incubation with the nanoparticle suspension at 37°C. Cells were then washed in serum-free RPMI medium and complete cell internalization of nanoparticles followed in a 30-min chase.

Stress-Induced Transfer of the Magnetic Label

After magnetic labeling of donor cells, cellular stress and the subsequent microvesicle release were induced by a 2-day incubation period in serum-deprived medium. Naïve recipient cells were thereafter incubated for 24 h at 37°C with the conditioned starvation medium in which donor cells were previously cultured. The following donor → recipient pairs were investigated: THP-1 → HUVEC, THP-1 → MSC, THP-1 → THP-1, HUVEC → THP-1, MSC → HUVEC and MSC → THP-1.

Single-Cell Magnetophoresis

In order to quantify the intercellular transfer of magnetic nanoparticles, we analyzed the magnetophoretic mobility of donor cells before and after starvation as well as the magnetophoretic mobility of recipient cells.

Quantification of cell magnetic load was performed by single cell magnetophoresis experiment as described previously (11). In brief, suspended labeled cells are submitted to a magnetic field gradient of known value. The magnetophoretic mobility of cells towards the magnet was recorded by videomicroscopy. The magnetic driving force acting on cells (M x grad B, where M is the cell magnetic moment and grad B is the magnetic field gradient) is balanced by the viscous force ($3\pi\eta dv$, where d is the cell diameter, v is the cell velocity and η is the medium viscosity). From the measurement of the velocity and diameter of each cell in the magnetic field (which was under our conditions 145 mT) and the magnetic field gradient of 17 mT/mm, we can calculate cell magnetization, which is proportional to the cell iron load. A magnetic moment of 6.6×10^{-14} A/m can be converted to 1 pg of iron. For each condition, the velocity and diameter of 100 cells were measured, yielding to the distribution of iron load per cell population.

Magnetic Resonance Imaging (MRI)

MRI was performed using a 4.7 T preclinical MRI system (BioSpec 47/40 USR, Bruker) in the Small Animal Imaging Platform Paris – Descartes PARCC-HEGP. High resolution MRI was carried out using a cryogenic probe (CryoProbe™, Bruker) in 0.3% low-melting-point agarose gels spiked with either donor or recipient cells (1×10^4 cells/mL).

Scans were run under a Fast Steady State Precession (FISP) protocol on FID mode. Images were acquired with the following parameters: FOV of $9\times9\times9$ mm; matrix of 180×180; voxel size of $50\times50\times50$ µm; echo time of 10 ms, repetition time of 20 ms; flip angle of 25° and bandwidth SW of 50 kHz.

Additionally, fast low-angle shot (FLASH) susceptibility weighted imaging (SWI) was performed. Typical parameters were: FOV of 1 cm x 0. 9 mm; matrix of 256×231; pixel of 39×39 µm; slice of 500 µm; echo time of 20 ms; repetition time of 750 ms; flip angle of 50° and bandwidth SW of 25 kHz.

Flow Cytometry

The impact of magnetic labeling and starvation stress on donor cell viability was investigated by flow cytometry analysis using an annexin V/propidium iodide assay kit (Sigma) according to the manufacturer's instructions. Cells were trypsinized and resuspended in binding buffer [10 mM HEPES, 140 mM NaCl, 2.5 mM CaCl2 (pH 7.4)] at a concentration of about 5×10^5 cells/mL. Annexin V-FITC and propidium iodide solutions were then added as directed by the manufacturer. Incubation was carried out for 15 min at room temperature in the dark. After, the cells were analysed by flow cytometry within 1 h. The following controls were used to set up compensation and quadrants for staining controls: unstained cells, cells stained with annexin V-FITC alone, cells stained with propidium iodide alone, and cells stained with both indicators. Flow-cytometric analysis of cells was performed using an CyAn ADP LX (Beckman Coulter) flow cytometer instrument (Flow Cytometry platform ImagoSeine - Institut Jacques Monod). Data were plotted on two-axis design, which had four quadrants. Quadrant R18 quantified population of dead but non-apoptotic cells (annexin-V negative and propidium iodide positive) while quadrant R19 indicated the population of late apoptotic cells (positive for both annexin-V and propidium iodide). Quadrant R21 concerned cells at the onset of apoptosis (stained positive for annexin-V alone) whereas the quadrant R20 represented viable cells (negative for both annexin-V and propidium iodide). Cell size and granularity were assessed by measuring mean forward scattering and mean side scattering, respectively. Donor cells were analysed before and after magnetic labeling and following the 2-day period of starvation stress.

Transmission Electron Microscopy

Cells were rinsed and fixed with 5% glutaraldehyde in 0.1 mol/L sodium cacodylate buffer, post fixed with 1% osmium tetroxide containing 1.5% potassium cyanoferrate. Cells were then gradually dehydrated in ascending concentrations of ethanol and embedded in Epon resin. Thin sections (70 nm) of cells were examined with a Zeiss EM 902 transmission electron microscope at 80 kV (platform MIMA2, INRA, Jouy-en-Josas, France). The fraction of interest of the conditioned starvation medium of labeled cells was also analysed by TEM. This fraction was obtained

in the following way: the medium was first centrifuged to eliminate dead cells and the largest apoptotic bodies. Then, the supernatant containing microvesicles was submitted to magnetic sorting processes, in order to isolate the magnetic fraction. The fraction attracted on the magnet was fixed and embedded for TEM observation.

Prussian Blue Staining

Prussian blue staining was used to reveal the presence of iron inside the cells. Cells were fixed in 10% formalin saline for 1 h, rinsed and incubated for 30 min with 2% potassium ferrocyanide in 3.7% hypochloric acid and rinsed again.

Confocal Microscopy

Magnetically-labeled macrophages were fluorescently labeled with pKH67 Green Fluorescent Cell Linker (Sigma) following manufacturer's instructions and cultured in serum-free RPMI medium. Naïve macrophages adhering on glass lamellae were labeled with CellMask Deep red plasma membrane stain (Invitrogen) following manufacturer's instructions. The conditioned medium of magnetically-labeled green-fluorescent macrophages was recovered after a 2-day culture in serum-free medium and incubated for 24 h with red-fluorescent naïve macrophages. Cells were then fixed with 4% formaldehyde in PBS for 10 min at 37°C.

Optical sections were acquired with the Olympus JX81/BX61 Device/Yokogawa CSU Device spinning disk microscope (Andor Technology plc, Belfast, Northern Ireland), equipped with a 60xPlan-ApoN oil objective lens (60x/1.42 oil, Olympus). Fluorescence was excited with an air-cooled ion laser at 488 nm for pkH67 green and at 543 nm for CellMask Deep red. Fluorescence emission was collected with filters at 525 nm for pkH67 green and at 685 nm for CellMask Deep red. No autofluorescence from macrophages was detected at these wavelengths under used laser power. All images were recorded under laser power and constant integration times. Three-dimensional reconstructions of optical sections were made with Andor IQ 1.8.1 software (Andor technology plc).

RESULTS

Validation of Cell Magnetic Labeling and Viability

Single cell magnetophoresis experiment demonstrated the efficient uptake of magnetic nanoparticles by the three types of cells - THP-1 macrophages, HUVEC and MSC – after 30 min incubation with citrate-coated nanoparticles ([Fe] = 10 mM). As illustrated in Figs. 1a and 2a, labeled cells showed a magnetophoretic mobility when subjected to a magnetic field gradient. The measurement of velocity and diameter for each cell gave access to the whole distribution of iron load per cell population (Figs. 1a and 2a). The iron content distribution for THP-1 macrophages and MSC revealed a higher nanoparticle uptake compared to HUVEC, due to their smaller size (4). The average iron uptakes ($m \pm \Delta m$) are given in Table I. The uptake dispersion $\Delta m/m$ among each cell population was about 45%.

Magnetic properties of labeled cells were also assessed by high resolution MRI scans of agarose phantoms containing a density of 10^4 cells/mL (Figs. 3a and 4a). As expected, control phantoms containing non-labeled cells showed a homogeneous MR signal corresponding to the MR signal of agarose alone. In contrast, well-defined signal voids ("black spots") were observed in both 3D FISP and 2D SWI scans of agarose phantoms containing magnetically-labeled cells. Iron oxide nanoparticles accumulated in intracellular compartments of labeled cells and locally distorted the magnetic field, causing dephasing of spins, therefore generating signal voids in T2*-weighted sequences. Susceptibility artefacts with barbell-like shape were clearly observed in SWI scans, while punctual signal voids were observed using 3D FISP sequence. These signals corresponded to single cells. The density of detected signal voids was similar for magnetically-labeled THP-1 and MSC phantoms, but clearly lower for labeled HUVEC although the same number of cells was dispersed in the gel. This indicates that some of the labeled HUVEC were not detected by MRI due to insufficient magnetic load. This finding is consistent with magnetophoresis results, showing a lower nanoparticle uptake by HUVEC compared to THP-1 and MSC.

TEM observations also confirmed the effective internalization of magnetic nanoparticles by the three types of cells and their confinement into intracellular lysosomes (Fig. 5). This finding is in agreement with previous studies demonstrating that citrate-stabilized magnetic nanoparticles are first adsorbed on the plasma membrane of any cell type by electrostatic interactions and are subsequently internalized by endocytotic pathway reaching lysosomes as ultimate compartments (4).

Flow cytometry analysis (Fig. 6) revealed that magnetic labeling did not affect cell size (mean forward scatter of 106.4 for labeled HUVEC *versus* 107.1 for non-labeled cells (Fig. 6a & d)), but induced an important increase in cell granularity (mean side scatter of 100.4 for labeled HUVEC *versus* 58.8 for non-labeled cells (Fig. 6a & d)) due to the scattering effect of intracellularly-confined nanoparticles. According to annexin V/propidium iodide assay (Fig. 6b), magnetic labeling did not reduce HUVEC nor MSC viable population. HUVEC viable population represented 84 and 87% of the analysed events before and after magnetic labeling, respectively (Fig. 6b and c). For MSC, the corresponding

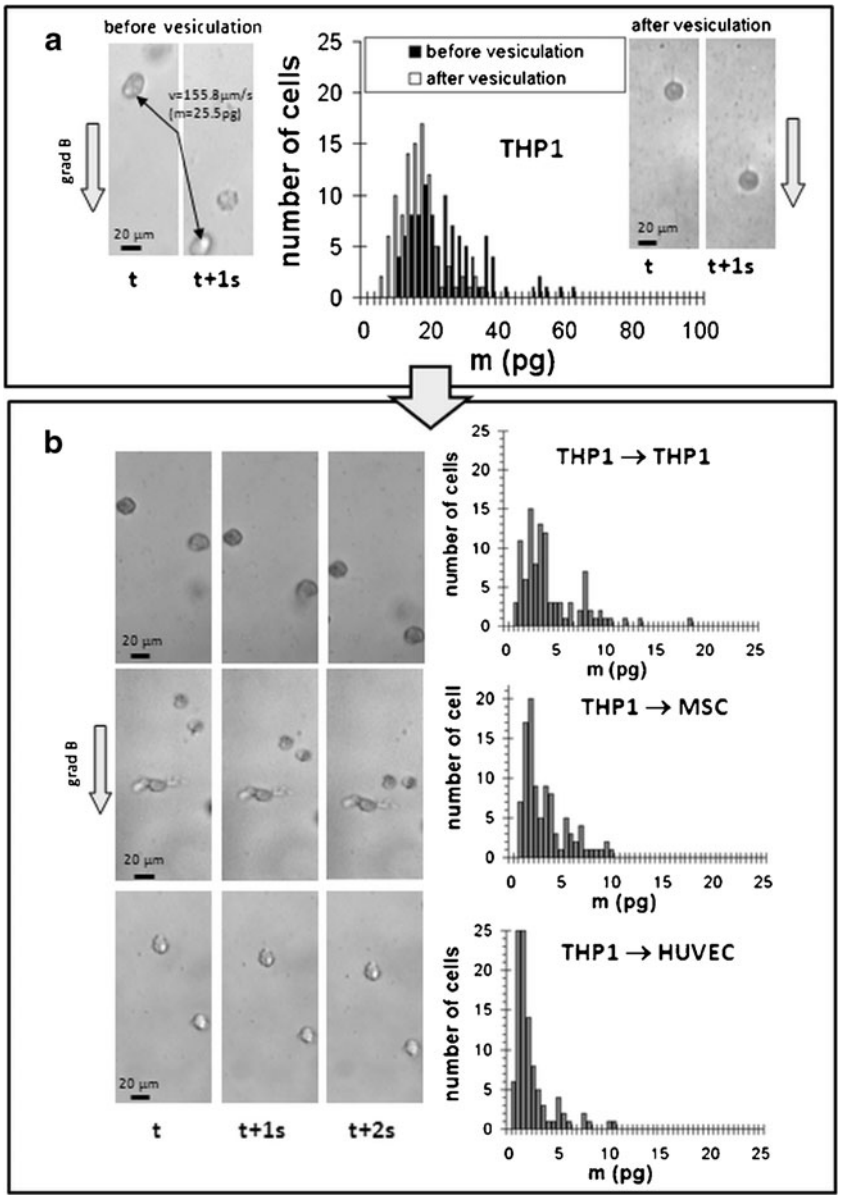

Fig. 1 Magnetophoretic mobility of labeled cells is shown in consecutive optical micrographs at different time points. *Black arrows* on the left couple of micrographs (**a**) point at the displaced cell moving in the direction of the magnetic field gradient with the velocity v in μm/s. The time lapse between two micrographs was 1 s. Intracellular iron mass distribution (m in pg), represented in the histograms (**a**) for donor THP-1 cells before and after stress-induced vesiculation and (**b**) for the following recipient cells - THP-1, MSC and HUVEC - incubated with THP-1 conditioned medium. (x → y legend indicates the pair of donor cells → recipient cells).

values were 85.5 and 83.4% (data not shown). Regarding THP-1 cells, only a small fraction (30%) of the total events were in the region corresponding to viable cells, even for the non-labeled cells. This may be related to the PMA treatment which on one hand induces differentiation of THP-1 monocyte cells into macrophages and on the other hand induces a high percentage of cell death and the presence of cell debris.

Stress Effect on Magnetically Labeled Cells

We next investigated the effect of the 2-day starvation stress period on cells labeled with magnetic nanoparticles (the donor cells). For all cell types, a decrease in magnetophoretic mobilities could be detected after starvation stress (Figs. 1a and 2a, Table I). The average intracellular iron mass was reduced by about 40% in stressed THP-1 and HUVEC, compared to the same cells prior starvation. The dispersion of cell iron load $\Delta m/m$ was also slightly reduced after starvation treatment (37%). Interestingly, the stress effect was far less pronounced for MSC showing only a 10% reduction in their iron load.

Apoptosis induced by starvation stress was assessed by FACS analysis using annexin V (AnnV)/propidium iodide (PI) assay on both non-labeled and labeled cells. For non-labeled HUVEC, stress slightly shifted viable cells to early apoptotic stages (6.8% Ann V +/PI- events *versus* 1.8% for non-stressed cells) and also induced cell death (7.4% Ann V -/PI + *versus* 1.9%) (Fig. 6b and c). For magnetically labeled HUVEC, the stress-induced shift to early apoptotic stage (Ann V +/PI-) was more marked (see Fig. 6b and c) representing 23.5% of the cell population *versus* 3.2% for the labeled non-stressed HUVEC.

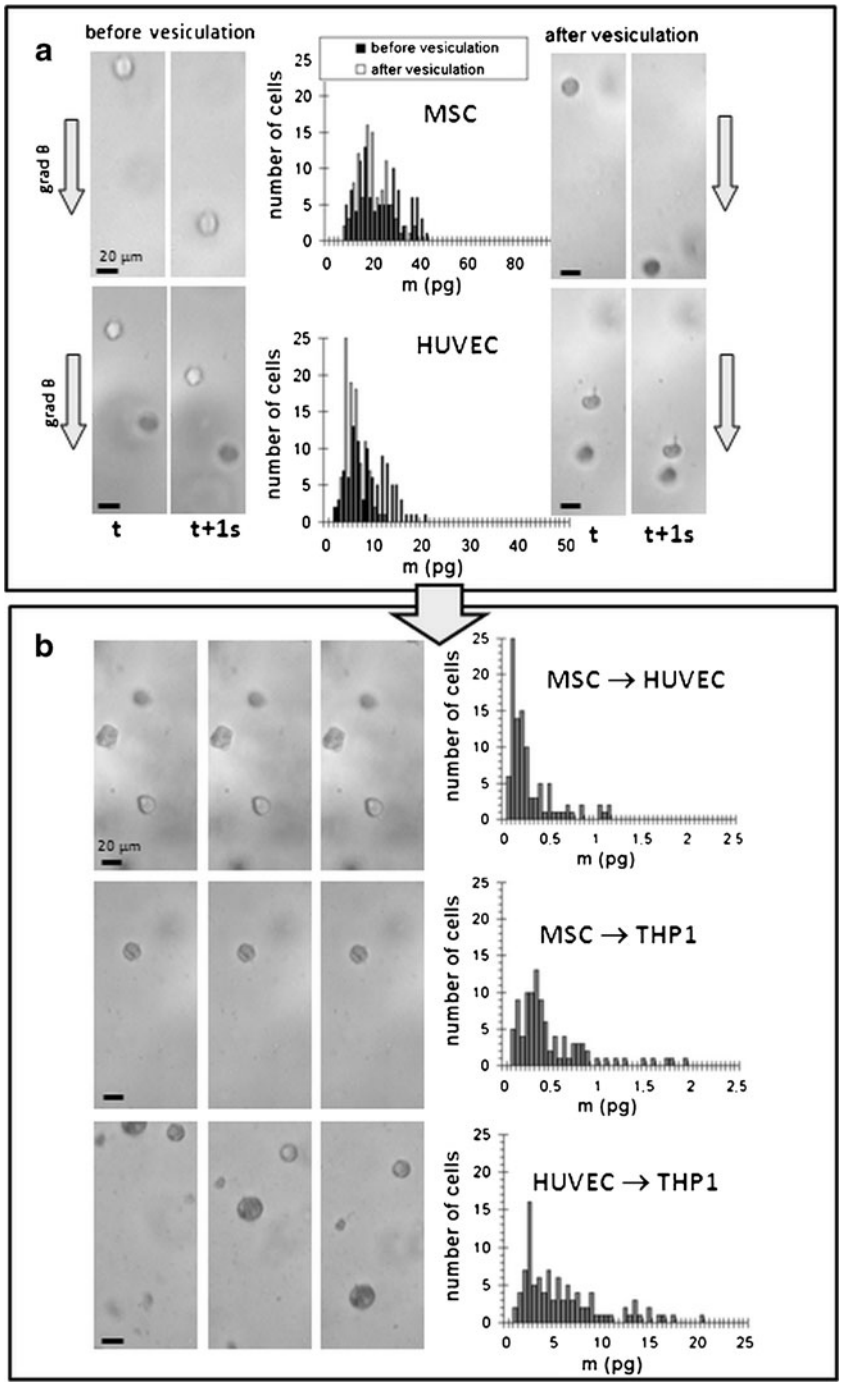

Fig. 2 Magnetophoretic mobility and intracellular iron mass distribution for donor MSC and HUVEC before and after stress-induced vesiculation (**a**) and for their following recipient cells - HUVEC and THP-1 – incubated with the donor cell conditioned medium (**b**).

However starvation stress had almost no effect on the viability of MSC, notwithstanding if they were labeled or not. The number of dead cells slightly rose, but early apoptotic cell population did not increase (data not shown). MSC resistance to stress was consistent with reduced impact of starvation on the cell iron load variation, as evidenced by magnetophoresis assay.

Table I Average Iron Uptake per Cell Line (in pg of Iron per cell)

Donor cell	Iron uptake m ± Δm (pg) before stress	Iron uptake m ± Δm (pg) after stress
THP1	23.81 ± 10.87	15.72 ± 6.05
MSC	21.28 ± 9.46	19.31 ± 6.53
HUVEC	8.81 ± 4.10	5.19 ± 1.99

Vesicle-Mediated Transfer of Magnetic Nanoparticles from Donor to Recipient Cells

In order to evidence the loss of iron load from starved cells, we analysed their extracellular medium after starvation by

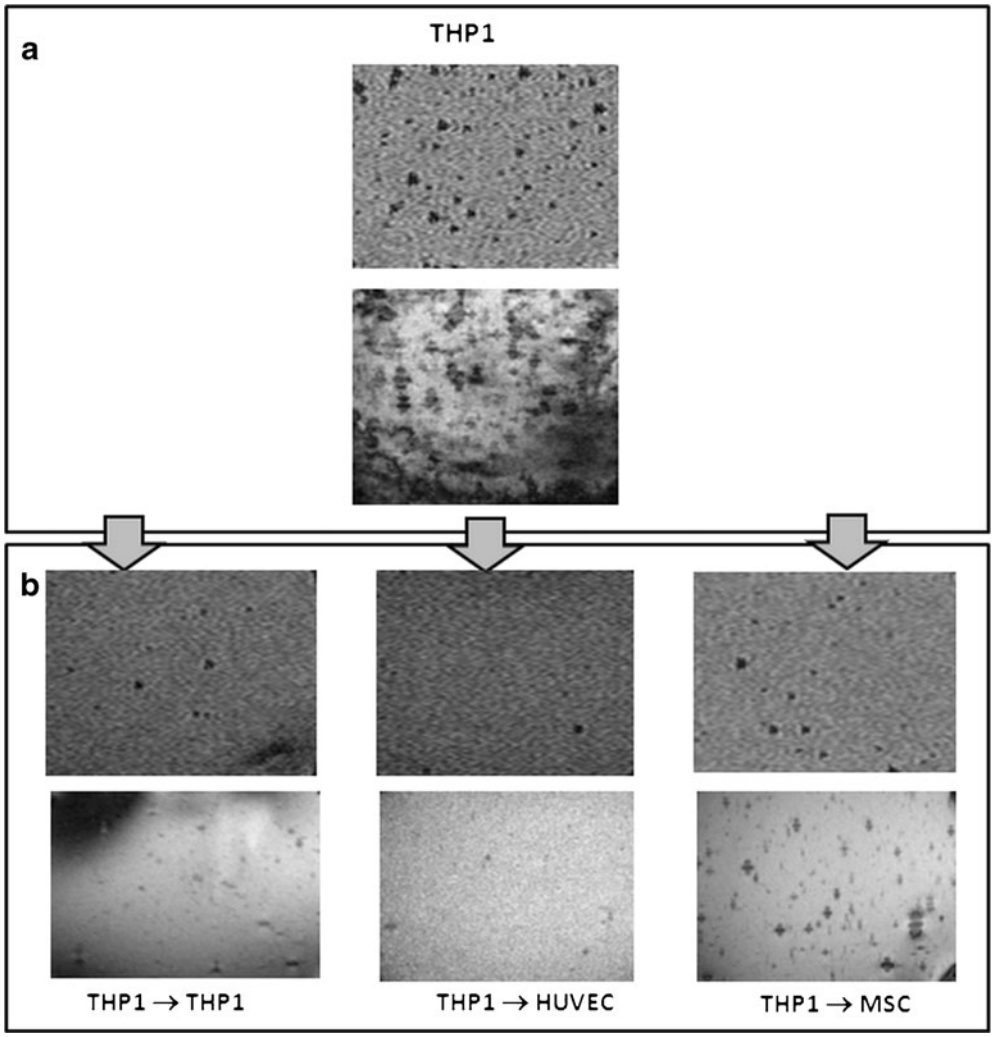

Fig. 3 High-resolution MRI scans of agarose phantoms containing THP-1 donor cells (**a**) and the following recipient cells - THP-1, HUVEC and MSC – incubated with the THP-1 conditioned medium (**b**). FISP scans (*top*) and SWI scans (*bottom*).

TEM (Fig. 7). This conditioned medium was subjected to a magnetic sorting in order to isolate the magnetic fraction. TEM observations of magnetic fraction revealed electron dense clusters of nanoparticles, most of them being enclosed in membrane compartments of vesicular structures. The release of nanoparticles from stressed THP-1 and HUVEC was mainly mediated by microvesicle shedding.

We next incubated naive recipient cells into the conditioned starvation medium of donor cells for 24 h and assessed the intercellular transfer of nanoparticles by single cell magnetophoresis and MRI of recipient cells.

For all investigated donor → recipient pairs, we observed a magnetophoretic mobility of recipient cells (Figs. 1b and 2b) demonstrating the effective cell relocation of nanoparticles. Quantitatively, indeed, the iron load of recipient cells strongly depended on the release from donor cells. The average iron contents of recipient cells as function of donor cell type are given in Table II. The poor translocation of nanoparticles from donor MSC can be correlated with their small decrease in iron load after starvation. Note that the iron load dispersion in recipient cells is much larger than that of directly-labeled donor cells, varying from 70% to 115%.

MRI data (Figs. 3b and 4b) were consistent with magnetophoresis results. For both FISP and SWI scans, signal voids were scarcely observed on phantoms of HUVEC or THP-1 incubated with MSC conditioned medium while they were quite abundant for THP-1 incubated with THP-1 or HUVEC conditioned medium.

The transfer of magnetic label from donor cells to naïve recipient cells could also be evidenced by microscopy after Perl's staining (Fig. 8a). Blue stain for iron-positive cells was widely observed in analyzed samples of naïve recipient cells. Inter-cell heterogeneity of iron content was evidenced, in agreement with the broad intracellular iron mass distribution for the recipient cell population indicated by magnetophoresis.

To investigate the role of membrane vesicles in intercellular transfer of magnetic nanoparticles, we first labeled the donor magnetic THP-1 with a green membrane marker and

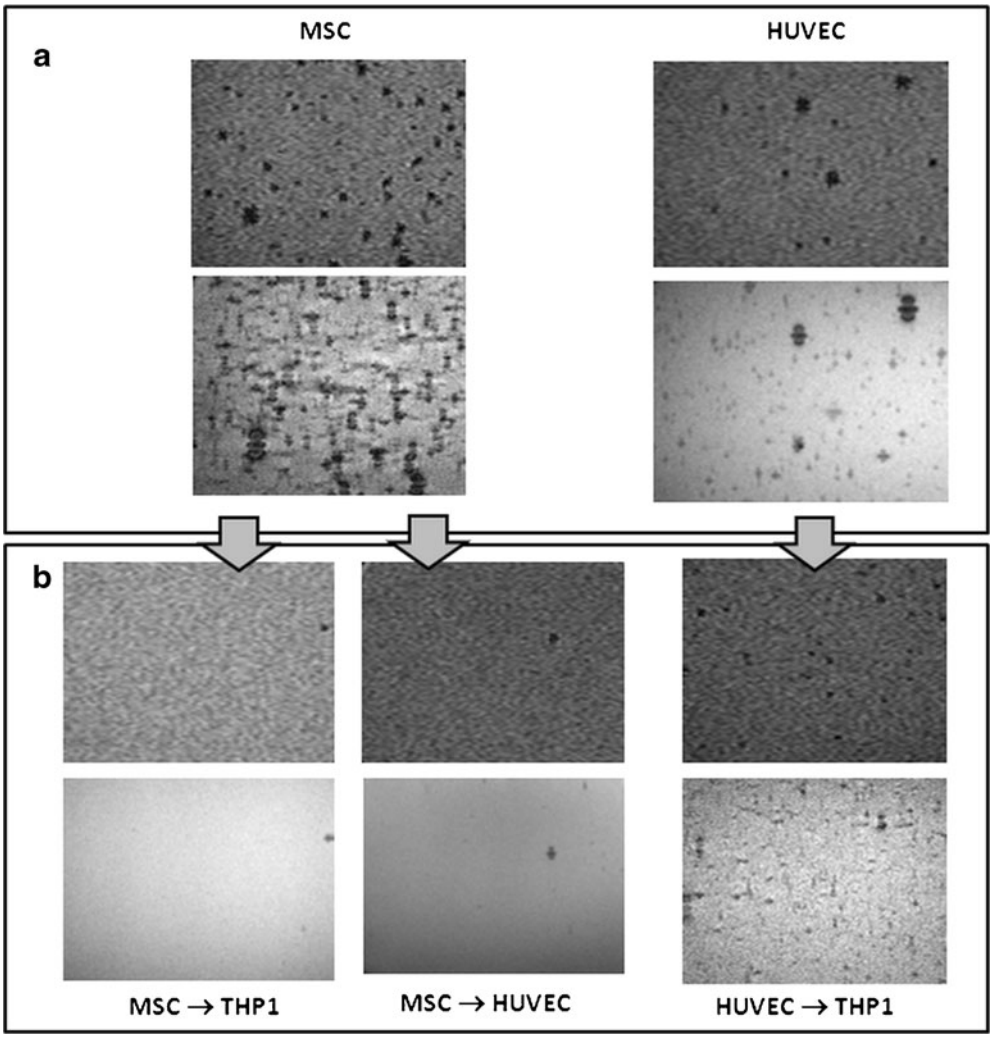

Fig. 4 High-resolution MRI scans of agarose phantoms containing MSC and HUVEC donor cells (**a**) and the following recipient cells: HUVEC and THP-1 (**b**). FISP scans (*top*) and SWI scans (*bottom*).

then transferred their conditioned medium to naïve macrophages. On the other part, naïve recipient macrophages were distinguished by labeling with CellMask red plasma membrane stain. Confocal microscopy images of red recipient macrophages showed green fluorescent individual spots with mainly intracellular localization (Fig. 8b). This indicates that cell microvesicles containing donor cell membrane could interact with naïve cells, could be internalized and could transfer their nanoparticle cargo to the recipient cells.

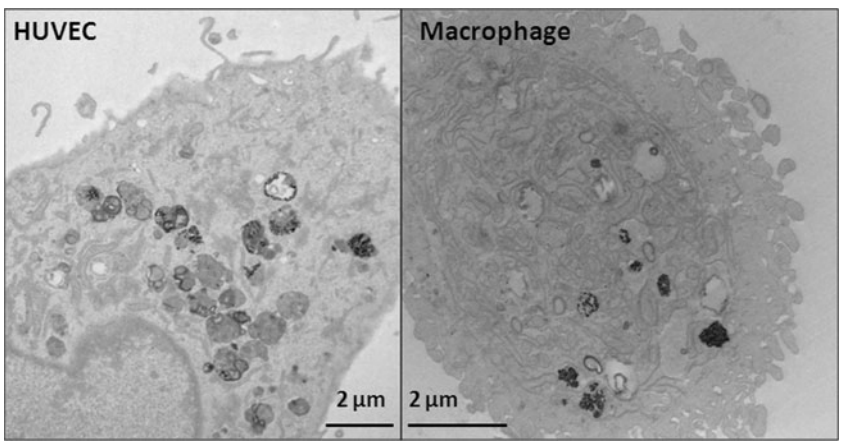

Fig. 5 TEM micrograph of HUVEC and THP-1-derived macrophages after labeling with citrate-coated iron oxide nanoparticles. Nanoparticles are confined into intracellular lysosomes.

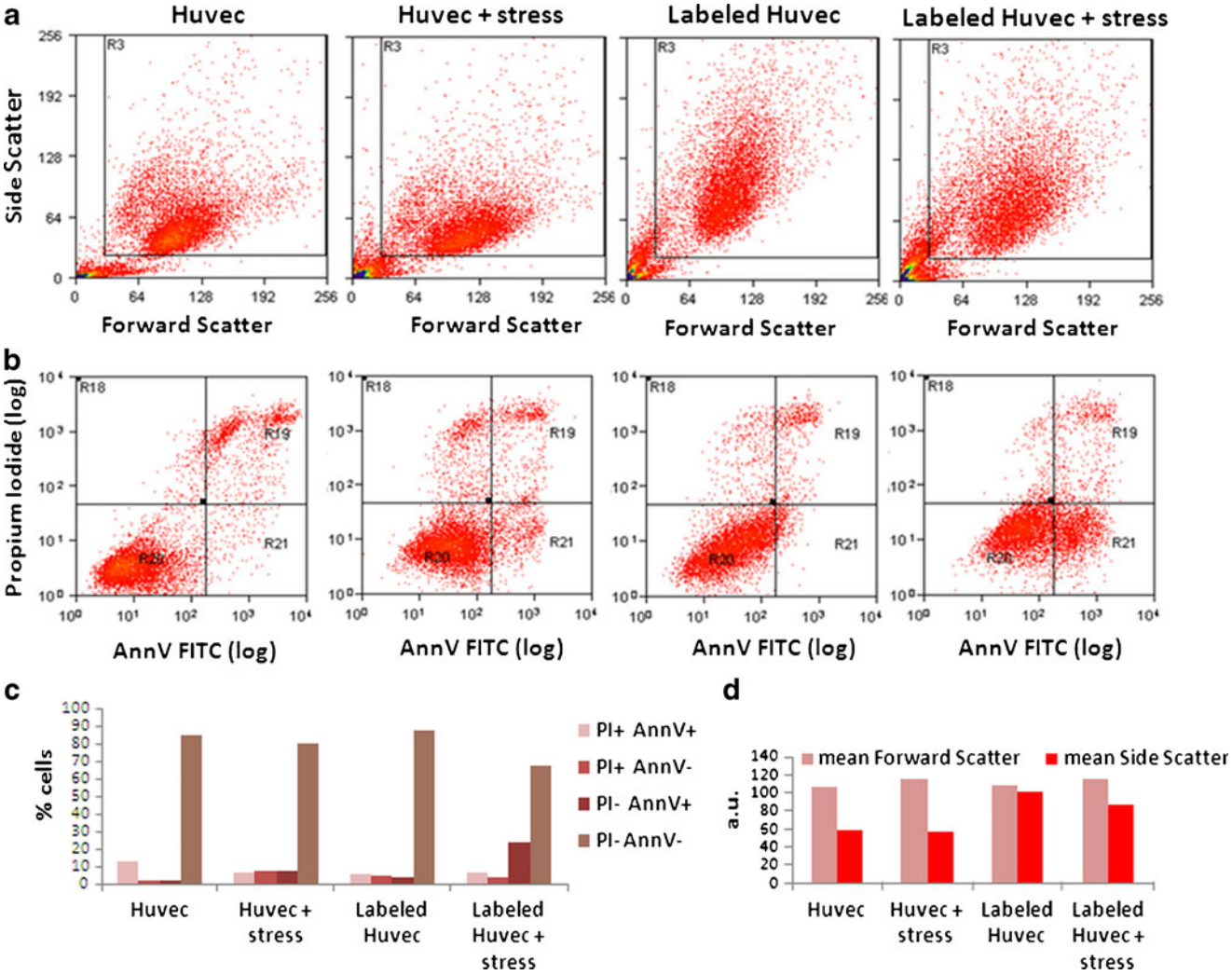

Fig. 6 Flow cytometry analysis of HUVEC before and after stress for both non-labeled and magnetically labeled cells. (**a**) Forward scattering × side scattering dual parameter scatter plots; (**b**) propidium iodide × Annexin V staining dual parameter scatter plots; (**c**) mean cell percentage for quadrants represented in B (R18: PI+/AnnV-; R19: PI+/AnnV+; R20: PI-/AnnV-; R21: PI-/AnnV+); (**d**) mean forward scattering and mean side scattering represented in A for quadrant R3.

DISCUSSION

Recent reports have questioned the specificity of magnetic labeling for tracking transplanted cells. For instance, Terrovitis *et al.* used xenogeneic and syngeneic rats with myocardial infarction injected with iron oxide- and/or β-galactosidase labeled murine or human BMSCs into the injured myocardium of rats. Histological analysis 3 weeks after transplantation revealed the presence of iron-containing macrophages at the injection site, identified by CD68 staining, but very few or no β-galactosidase–positive stem cells (5).

In a related study, Amsalen and colleagues investigated the effectiveness of transplantation of magnetically labeled mesenchymal stem cells in a rat model of myocardial infarction. They observed that 4 weeks after injection, most of the transplanted labeled MSCs did not survive. Using immunohistochemical staining, the authors showed that most of the Prussian blue positive cells for iron were infiltrating macrophages that participated in the rejection process (6). Pawelczyk *et al.* also showed that the implantation of iron oxide-labeled cells could result in the uptake of the label by activated macrophages. Transfer of iron to activated macrophages *in vitro* accounted for <10% of the total iron in labeled cells (12). The same group also performed *in vivo* tests and confirmed that direct implantation of labeled BMSCs into localized area of inflammation and angiogenesis, could result in non-specific uptake of the magnetic label by infiltrating local tissue macrophages (13).

Our study marks a step forward in the understanding of magnetic label transfer by evidencing the role of cell-released vesicles. Our findings comprise four main conclusions: (a)

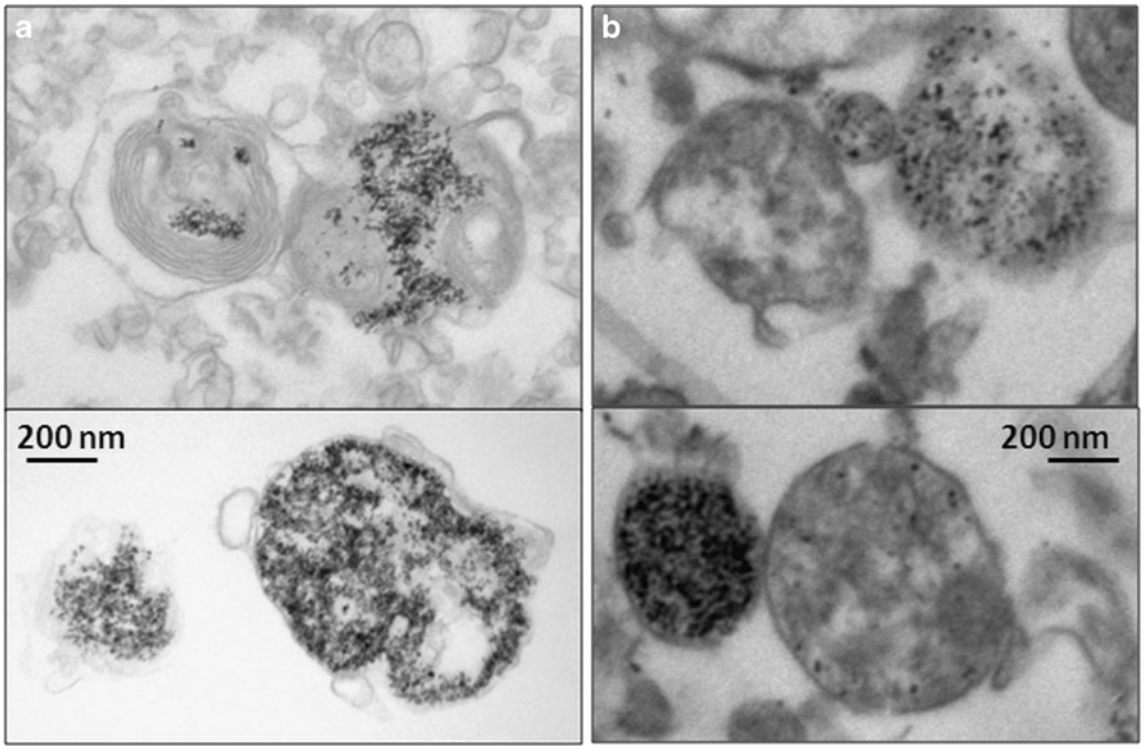

Fig. 7 Microvesicles released by HUVEC (**a**) and THP-1-derived macrophages (**b**) after 24 h of serum deprivation. The conditioned medium of HUVEC and macrophages was subjected to magnetic attraction before fixation for TEM. Nanoparticles are found enclosed in membrane vesicles.

magnetic label is partially lost under cell stress; (b) cell microvesicles participate in magnetic label release; (c) cell microvesicles are uptaken by naïve cells transferring the magnetic label; (d) intercellular transfer of nanoparticles is not limited to macrophages, but can also involve endothelial and stem cells as donor or recipient cells with different effectiveness.

Magnetic nanoparticle release under stress implied a decrease in the magnetic properties of donor cells. This was clearly demonstrated by comparing the magnetophoretic mobility of donor cells before and after starvation stress. In this concern, single-cell magnetophoretic experiment was found to be a very sensitive technique.

Table II Average Iron Contents of Recipient Cells in Relation to Different Donor Cells

Recipient cell	Donor cell conditioned medium	Iron uptake m ± Δm (pg)
THP1	HUVEC	5.78 ± 4.32
THP1	THP1	4.18 ± 2.99
MSC	THP1	3.17 ± 2.21
HUVEC	THP1	2.03 ± 1.92
THP1	MSC	0.53 ± 0.61
HUVEC	MSC	0.26 ± 0.26

The way cells respond to stress directly impacts the release of magnetic nanoparticles in cell microvesicles. As cell microvesicles are constitutively produced during stress or apoptosis, an increase in early apoptotic cell population would result in a more important loss of the magnetic label considering its release via cell microvesicles. This assumption was confirmed by the presented data. Compared to MSC, HUVEC underwent stress-induced apoptosis to a greater extent, according to FACS analysis. As a consequence, vesicle release carrying along the magnetic nanoparticles was more pronounced in HUVEC and resulted in an important intracellular iron mass reduction after starvation stress. This may be also related to the sensitivity of endothelial cells to various stress with a demonstrated ability to release high number of microvesicles in circulating blood (7–9). Interestingly, the high resistance of mesenchymal stem cells to starvation stress makes them less prone to nanoparticle release and subsequent intercellular transfer.

The role of cell microvesicles in nanoparticle release by magnetically labeled cells under stress was ascertained by analysing the conditioned medium obtained after starvation. TEM micrographs revealed nanoparticles enclosed in vesicular structures, clearly indicating that cell microvesicles are implicated in the loss of cell magnetization under cell stress.

Cell-released vesicles include cell microparticles, exosomes and apoptotic bodies. Cell microparticles are released

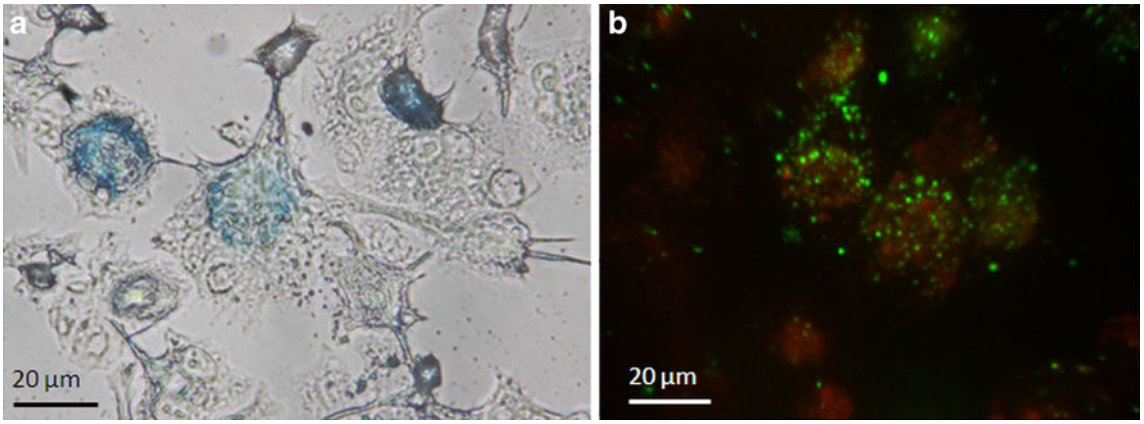

Fig. 8 Red-fluorescent naive macrophages incubated for 24 h with the conditioned medium of green-fluorescent magnetically-labeled macrophages. (**a**) Perls staining shows the transfer of iron-oxide nanoparticles into the naive macrophages. (**b**) Confocal imaging shows the uptake of green-fluorescent macrophage-released vesicles into the red-fluorescent naive macrophages.

from the cell membrane upon cell activation and early apoptosis. The liberation of cell microparticles occurs by a blebbing or shedding process, resulting in particles ranging from 100 to 1,000 nm in diameter. Apoptotic bodies are larger than cell microparticles (>1 µm) and contain remnants of the degradation processes of the shrinking apoptotic cells. The fragmentation of the apoptotic cell into bodies facilitates their clearance. Exosomes are derived from multivesicular bodies, and are smaller and more homogeneous in size, ranging from 40 to 100 nm in diameter. Multivesicular body fuse with the cell membrane leading to the release of compartments and exosomes from their parental cells (14,15).

Cell-released vesicles carry a broad variety of cytoplasmic and nuclear components, including both DNA and RNA (16). Our findings concerning the transfer of magnetic nanoparticles broadens the range of materials that are known to be transported by cell microvesicles. Precisely, these findings indicate that cell-derived vesicles are able to carry not only endogenous substances but also exogenous nanoparticles uptaken by cells. A similar role has already been evidenced for tumour cell-derived vesicles which carry along high concentrations of cytostatics contributing to multi-drug resistance (17).

Considering that cell microvesicles were implicated in the partial loss of magnetic label under cell stress, the next step was to investigate if they were able to transfer their cargo to naïve cells. For this, we analysed the magnetic properties of naïve cells that were incubated with the donor conditioned starvation medium. The results obtained from single-cell magnetophoresis indicated that naïve recipient cells indeed presented magnetophoretic mobility. Interestingly, intracellular iron load from naïve recipient cells was not directly related to the iron load from donor cells. For instance, although MSC presented a higher intracellular iron load compared to HUVEC, naïve recipient cells incubated with HUVEC conditioned medium displayed superior iron content than the ones incubated with MSC conditioned medium. As commented above, MSC resistance to starvation stress did not induce extended apoptosis, subsequently limiting vesicle release and magnetic label transfer. Intracellular iron load from naïve recipient cells may relate to the iron load from donor cells as long as the latter are stress responsive and apoptosis is triggered. This seems to be the case for THP-1 donor cells, but we cannot rely on FACS analysis to confirm this assumption.

While Pawelczyk *et al.*, considered that the hypointense signals from magnetically labeled host recipient cells would be below MRI detection level (12), we would like to warn that the transferred microvesicle-cargo cannot be ignored. In terms of MRI analysis, the contribution of transferred label, resulting in hypo-signal observed under our conditions in agarose phantoms containing naïve recipient cells, cannot be considered minimal. The extended presence of signal voids, mainly for THP-1 incubated with THP-1 or HUVEC conditioned medium supports this assertion. Indeed, cell tracking was, under our conditions, performed with a sensitive, high-field (4.7 T) MR scanner provided with a cryogenic probe, which is nowadays not available yet for clinical research. However, future advancements in clinical MRI seem to be moving towards high magnetic fields, which paves the way to higher MRI sensitivity in clinics, which will certainly open new frontiers for MRI cell tracking in humans. Based on our findings, we suggest that the transfer of magnetic nanoparticles via cell microvesicles from transplanted cells to host bystander cells (which is not limited to macrophages), may be detected by MRI and might lead to over-interpretation of results while tracking transplanted cells. Other than the implications on MRI cell tracking, the health impact related to the dissemination of the magnetic nanoparticles in the organism should be taken into account.

CONCLUSIONS

Our study marks a step forward in the understanding of intercellular transfer of magnetic nanoparticles. Besides confirming that magnetic label may be partially lost under cell stress, we demonstrate that cell microvesicles participate in the release of nanoparticles. Their subsequent uptake by naïve cells leads to a redistribution of the magnetic nanoparticles. To our knowledge, this is the first time that insight is provided into cell microvesicle role in the transfer of magnetic nanoparticles among different cell types. The obtained results support the assumption that implantation of magnetically labeled cells *in vivo* can result in non-specific uptake of the label by local host cells. Therefore, the presented data raise concern about the specificity and reliability of MRI in tracking the fate of magnetically labeled transplanted cells.

ACKNOWLEDGMENTS & DISCLOSURES

This work has been supported by the European project Magnifyco (Contract NMP4- SL-2009-228622). The authors thank Gwennhael Autret and Olivier Clément from the Small Animal Imaging Platform Paris – Descartes at the PARCC-HEGP for MRI imaging, Nicole Boggetto from the Flow Cytometry platform ImagoSeine - Institut Jacques Monod for FACS analysis, Christine Longin and Sophie Chat from Mima2 platform- Inra (Jouy en Josas) for TEM analysis and Pierre Emmanuel Rautou and Chantal Boulanger for fruitful discussion. J. Kolosnjaj-Tabi was supported by the European network ENCITE.

REFERENCES

1. Rogers WJ, Meyer CH, Kramer CM. Technology insight: *in vivo* cell tracking by use of MRI. Nat Clin Pract Cardiovasc Med. 2006;3(10):554–62.
2. Frank JA, Miller BR, Arbab AS, Zywicke HA, Jordan EK, Lewis BK, *et al.* Clinically applicable labeling of mammalian and stem cells by combining superparamagnetic iron oxides and transfection Agents1. Radiology. 2003;228(2):480–7.
3. Hinds KA, Hill JM, Shapiro EM, Laukkanen MO, Silva AC, Combs CA, *et al.* Highly efficient endosomal labeling of progenitor and stem cells with large magnetic particles allows magnetic resonance imaging of single cells. Blood. 2003;102(3):867–72.
4. Wilhelm C, Gazeau F. Universal cell labelling with anionic magnetic nanoparticles. Biomaterials. 2008;29(22):3161–74.
5. Terrovitis J, Stuber M, Youssef A, Preece S, Leppo M, Kizana E, *et al.* Magnetic resonance imaging overestimates ferumoxide-labeled stem cell survival after transplantation in the heart. Circulation. 2008;117(12):1555–62.
6. Amsalem Y, Mardor Y, Feinberg MS, Landa N, Miller L, Daniels D, *et al.* Iron-oxide labeling and outcome of transplanted mesenchymal stem cells in the infarcted myocardium. Circulation. 2007;116(11):138–45.
7. Pap E, Pallinger E, Pasztoi M, Falus A. Highlights of a new type of intercellular communication: microvesicle-based information transfer. Inflamm Res. 2009;58(1):1–8.
8. Leroyer AS, Tedgui A, Boulanger CM. Role of microparticles in atherothrombosis. J Intern Med. 2008;263(5):528–37.
9. Chironi GN, Boulanger CM, Simon A, Dignat-George F, Freyssinet JM, Tedgui A. Endothelial microparticles in diseases. Cell Tissue Res. 2009;335(1):143–51.
10. Luciani N, Wilhelm C, Gazeau F. The role of cell-released microvesicles in the intercellular transfer of magnetic nanoparticles in the monocyte/macrophage system. Biomaterials. 2010;31(27):7061–9.
11. Wilhelm C, Gazeau F, Bacri JC. Magnetophoresis and ferromagnetic resonance of magnetically labeled cells. Eur Biophys J. 2002;31(2):118–25.
12. Pawelczyk E, Arbab AS, Chaudhry A, Balakumaran A, Robey PG, Frank JA. *In vitro* model of bromodeoxyuridine or iron oxide nanoparticle uptake by activated macrophages from labeled stem cells: implications for cellular therapy. Stem Cells. 2008;26(5):1366–75.
13. Pawelczyk E, Jordan EK, Balakumaran A, Chaudhry A, Gormley N, Smith M, *et al. In vivo* transfer of intracellular labels from locally implanted bone marrow stromal cells to resident tissue macrophages. PLoS One. 2009;4(8):e6712.
14. Beyer C, Pisetsky DS. The role of microparticles in the pathogenesis of rheumatic diseases. Nat Rev Rheumatol. 2009;6(1):21–9.
15. Morel O, Toti F, Hugel B, Freyssinet JM. Cellular microparticles: a disseminated storage pool of bioactive vascular effectors. Curr Opin Hematol. 2004;11(3):156–64.
16. Valadi H, Ekström K, Bossios A, Sjöstrand M, Lee JJ, Lötvall JO. Exosome-mediated transfer of mRNAs and microRNAs is a novel mechanism of genetic exchange between cells. Nat Cell. 2007;9(6):654–9.
17. Safaei R, Larson BJ, Cheng TC, Gibson MA, Otani S, Naerdemann W, *et al.* Abnormal lysosomal trafficking and enhanced exosomal export of cisplatin in drug-resistant human ovarian carcinoma cells. Mol Cancer. 2005;4(10):1595–604.